Electronic Supplementary Material (ESI) for Journal of Materials Chemistry C.

Supplementary Information

Diketopyrrolopyrrole-based conjugated polymers containing planar benzo[*c*]cinnoline and tetraazapyrene structures for high-performance and long-term stable triboelectric nanogenerator

Kuang-Hao Cheng[a], Cheng-You Tsai[a], Yu-Han Wang[a], Shyam S. Pandey[b], Chih-Yu Chang[a]**, Jyh-Chien Chen[a]*

[a]*Department of Materials Science and Engineering, National Taiwan University of Science and Technology, Taipei, 10607, Taiwan.*
[b]*Graduate School of Life Science and Systems Engineering, Kyushu Institute of Technology, 2-4 Hibikino, Wakamatsu, Kitakyushu 808-0196, Japan.*

***E-mail: cychang@gapps.ntust.edu.tw *E-mail: jcchen@mail.ntust.edu.tw*

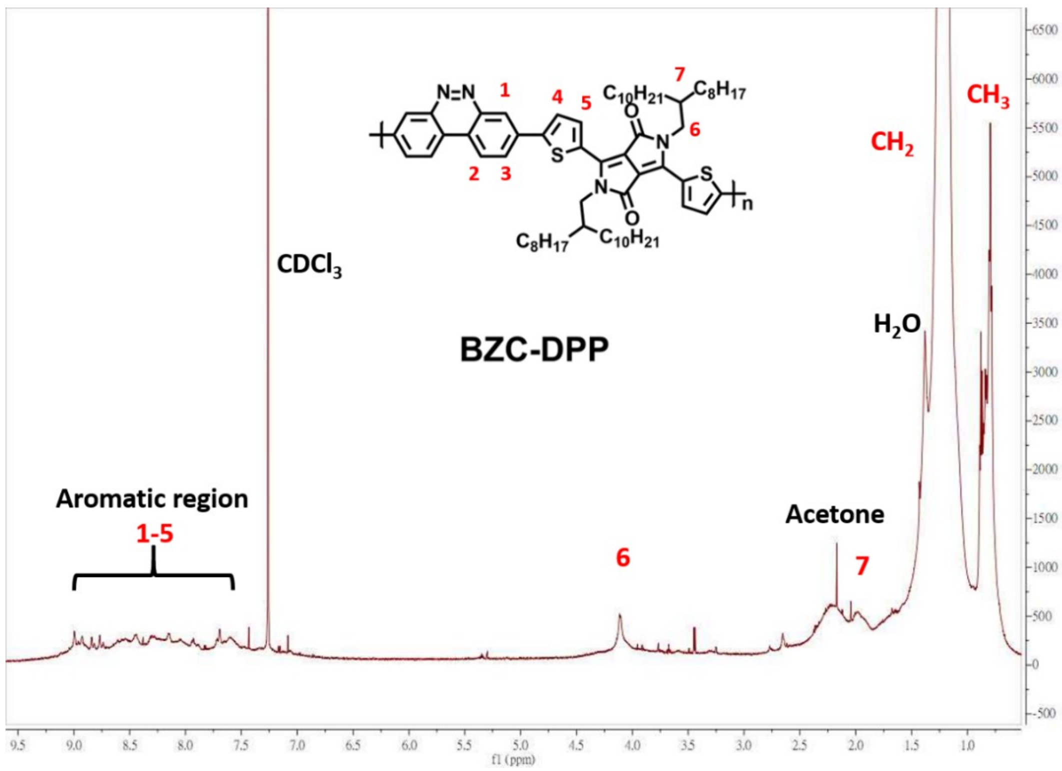

Fig. S1 ^{1}H NMR spectrum of BZC-DPP in $CDCl_3$.

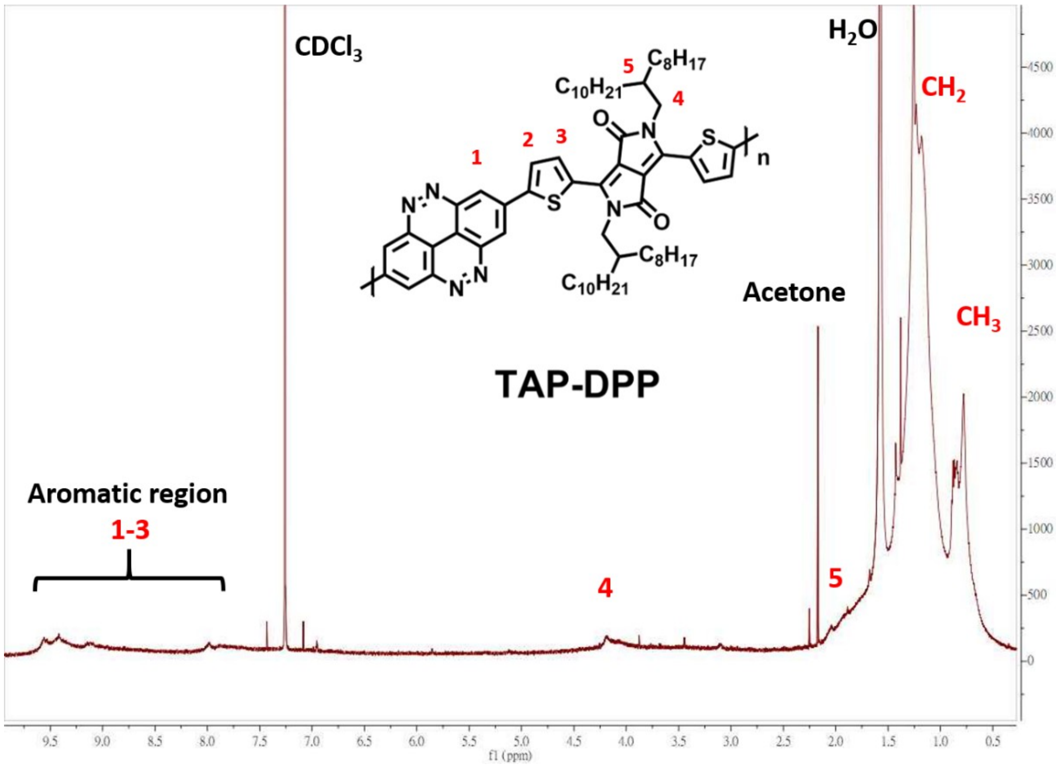

Fig. S2 ^{1}H NMR spectrum of TAP-DPP in $CDCl_3$.

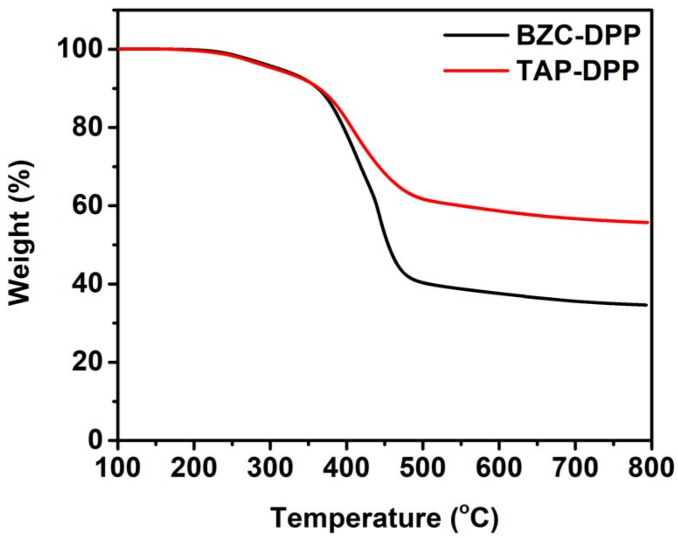

Fig. S3 TGA curves of BZC-DPP and TAP-DPP.

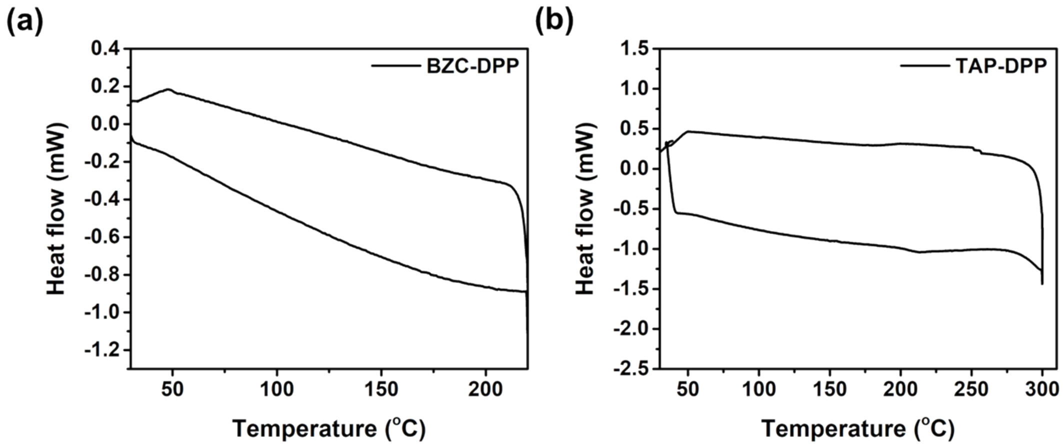

Fig. S4 DSC curves of (a) BZC-DPP and (b) TAP-DPP.

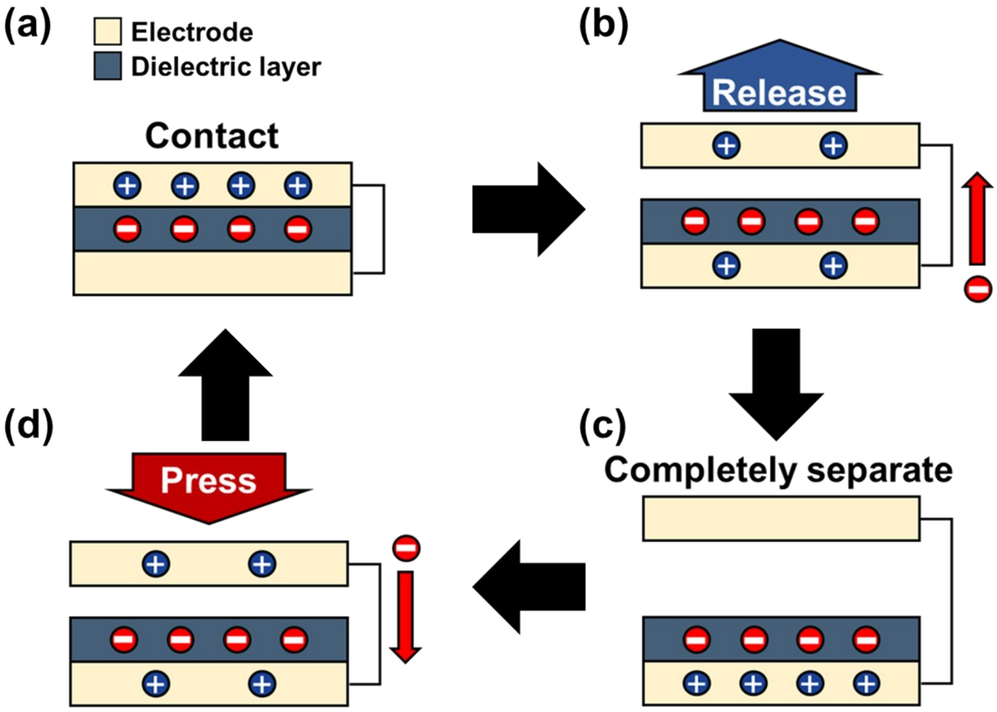

Fig. S5 Schematic illustration of the working principle of the metal-dielectric contact separation mode TENG.

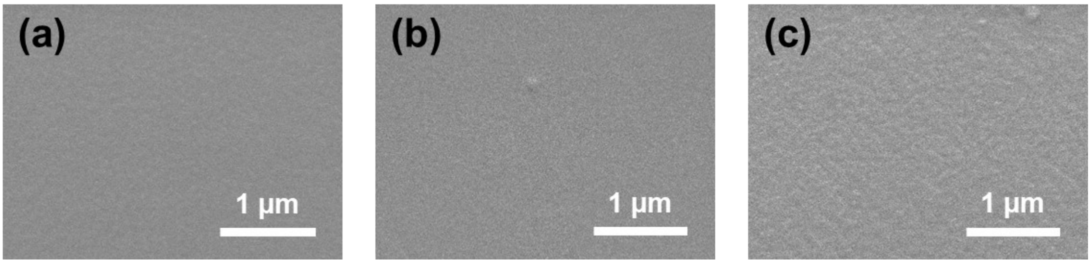

Fig. S6 Top-view SEM image of dielectric layer: (a) pristine PDMS, (b) PDMS/BZC-DPP, and (c) PDMS/TAP-DPP.

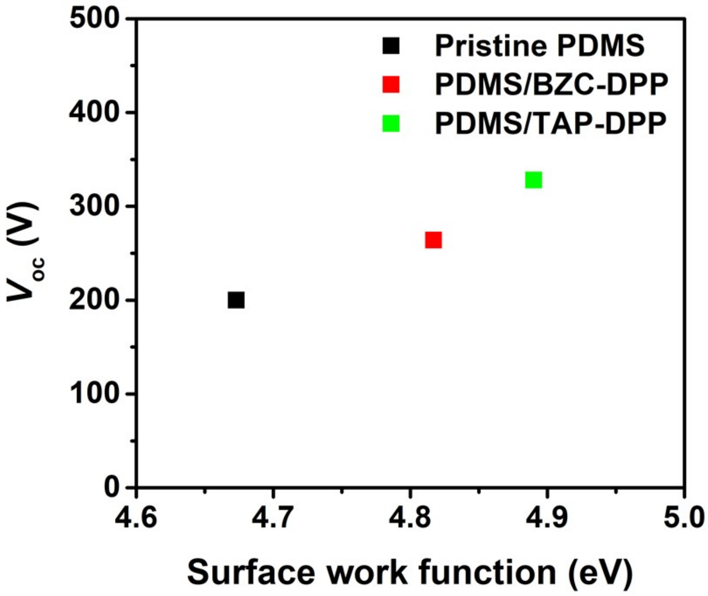

Fig. S7 Dependence of WF values and the corresponding V_{oc} output based on different modification layers.

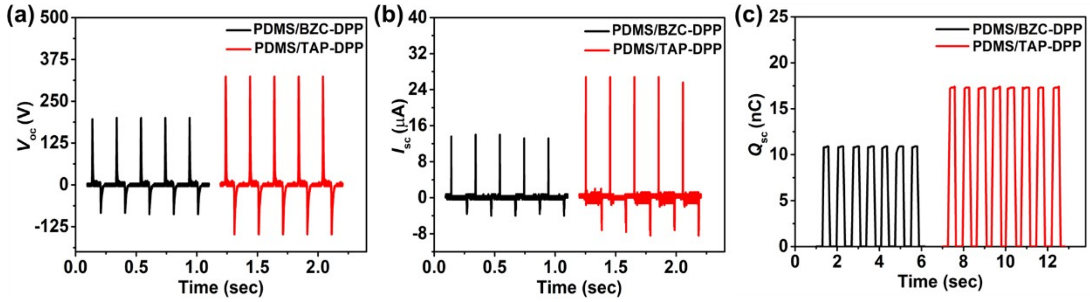

Fig. S8 Output characteristics of the TENG with 20-nm-thick DPP polymer layer: (a) V_{oc}, (b) I_{sc}, and (c) Q_{sc}.

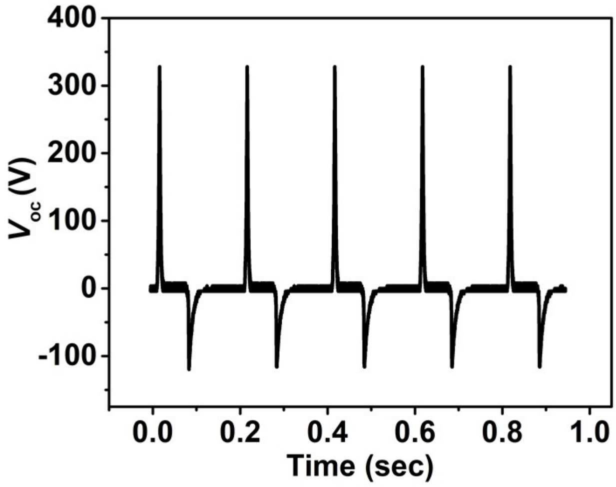

Fig. S9 V_{oc} output of the TENG after exposure to high humidity (95% relative humidity) for 1 hour.

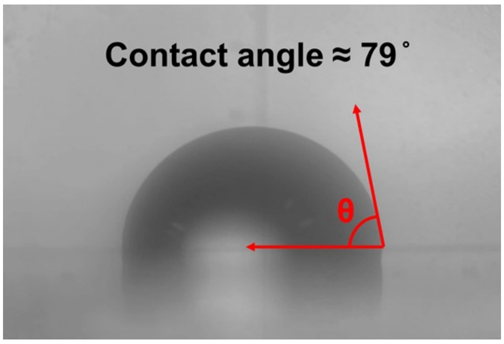

Fig. S10 Photograph of water contact angle analysis of PDMS/TAP-DPP.

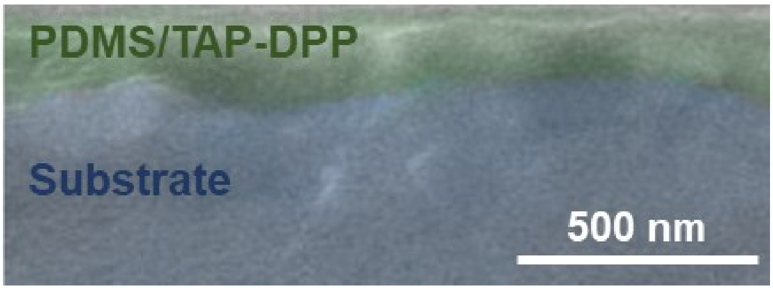

Fig. S11 Cross-sectional SEM image of PDMS/TAP-DPP film after continuous operation for 200,000 cycles.

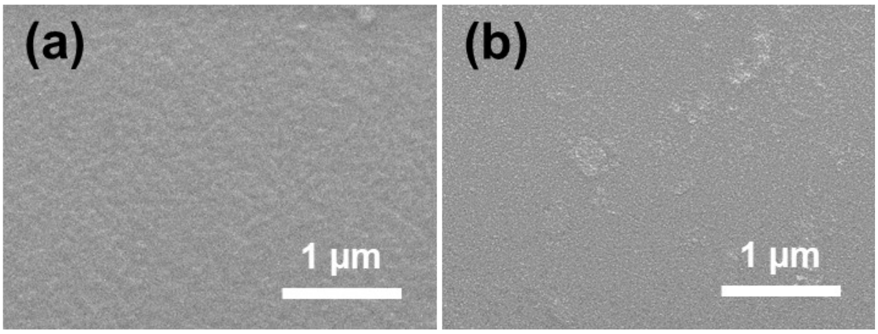

Fig. S12 Top-view SEM image of PDMS/TAP-DPP film: (a) before, (b) after continuous operation for 200,000 cycles.

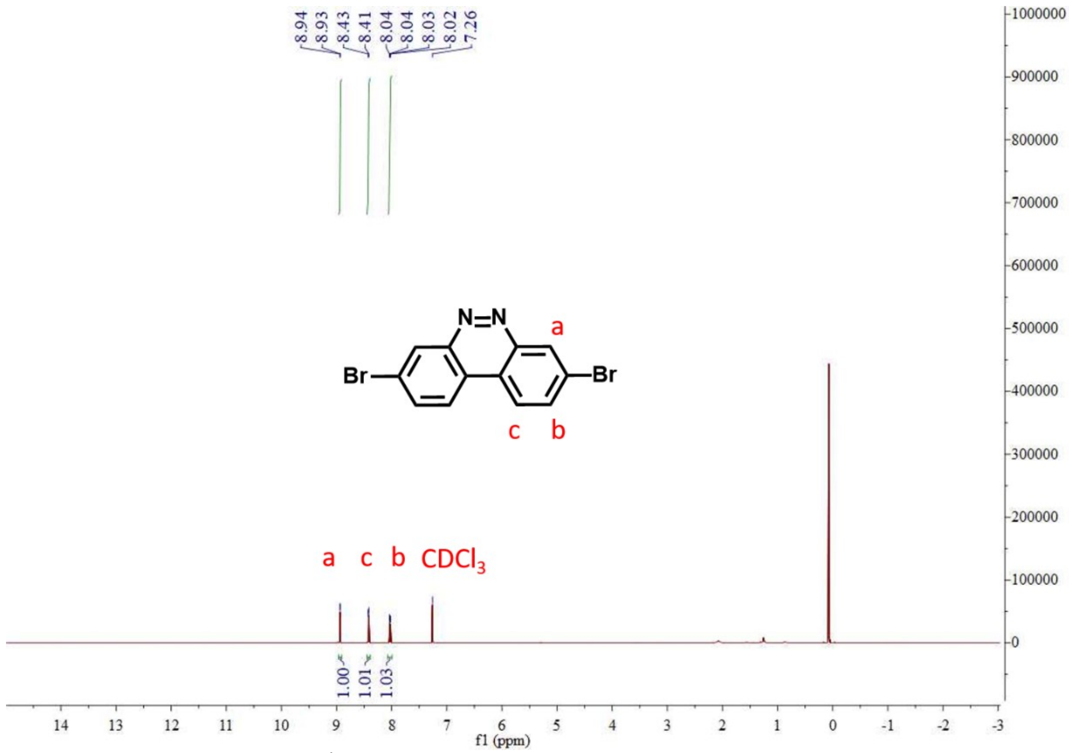

Fig. S13 ^{1}H NMR spectrum of compound **(3)** in $CDCl_3$.

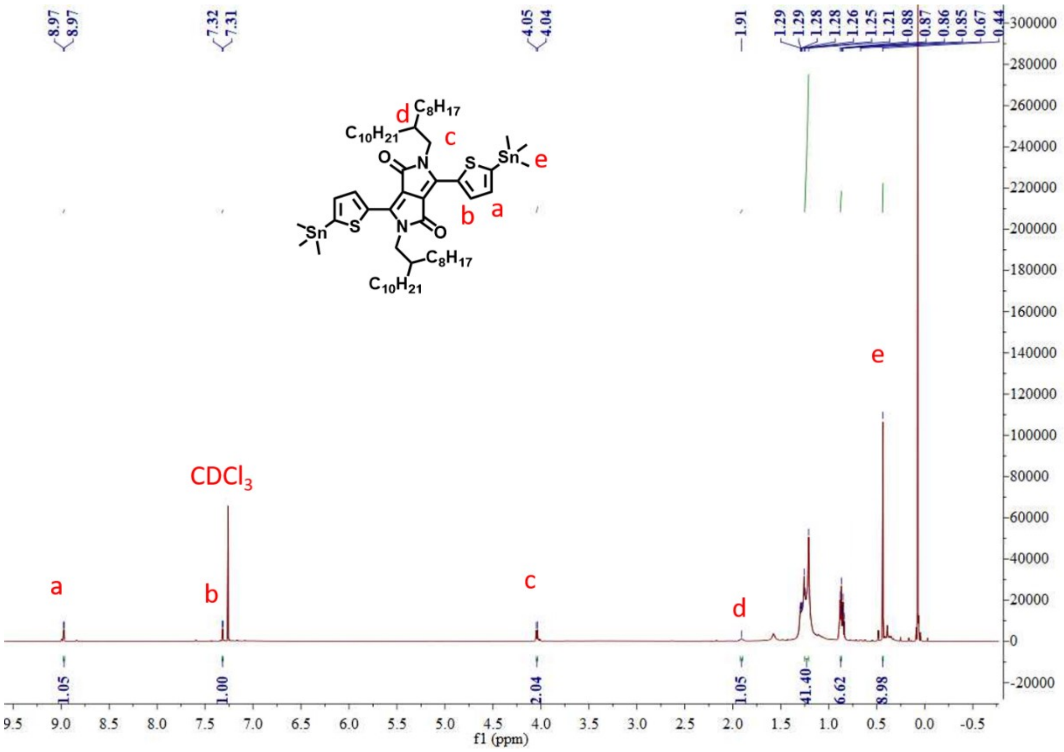

Fig. S14 ^{1}H NMR spectrum of compound **(6)** in $CDCl_3$.

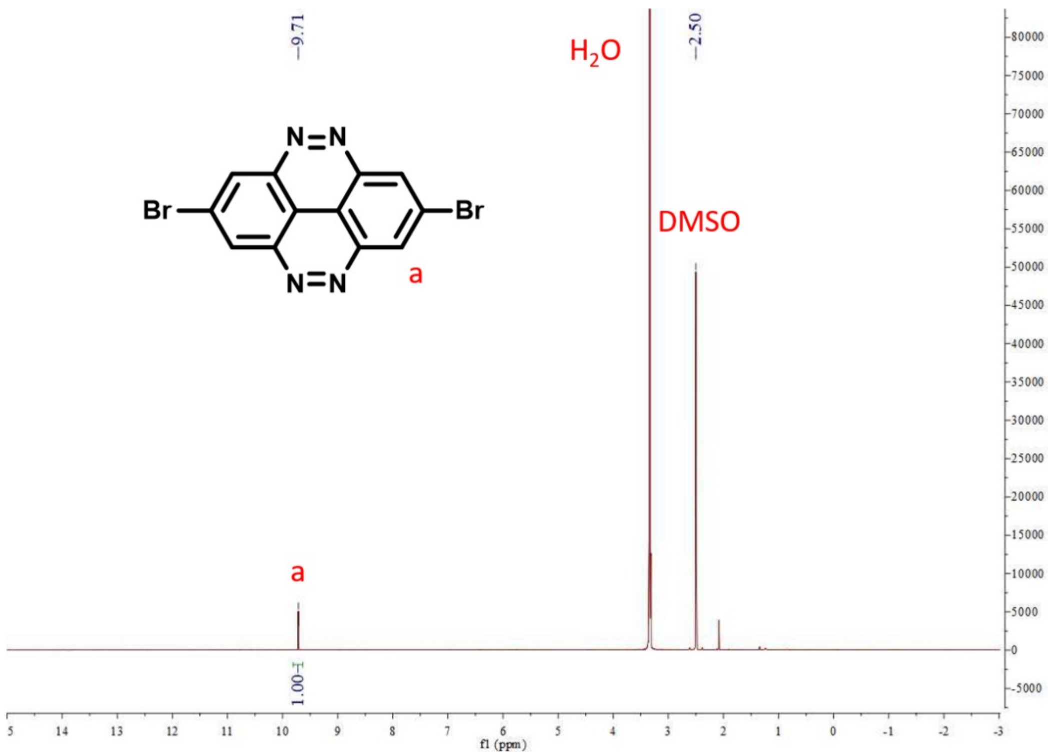

Fig. S15 ^{1}H NMR spectrum of compound **(12)** in DMSO.

Table S1 The decomposition temperatures of BZC-DPP and TAP-DPP

	$Td_{5\%}$ (°C)	$Td_{10\%}$ (°C)	Char yield (%)
BZC-DPP	312	362	35
TAP-DPP	306	363	56

Table S2 Summary of the output characteristics of the TENG with different thickness of DPP polymers. The values in parentheses are the best-performing TENG

Dielectric layer	DPP polymer thickness [nm]	V_{oc} [V][a]	I_{sc} [μA][b]	Q_{sc} [nC]
PDMS/BZC-DPP	10	248.8 ± 8.2 (264)	22.4 ± 0.6 (23.4)	13.9 ± 0.3 (14.4)
PDMS/TAP-DPP	10	313.6 ± 7.4 (328)	26.3 ± 0.4 (27.0)	17.9 ± 0.4 (18.5)
PDMS/BZC-DPP	20	198.2 ± 1.8 (200)	13.9 ± 0.1 (14.0)	10.8 ± 0.1 (10.9)
PDMS/TAP-DPP	20	319.8 ± 4.4 (324)	25.9 ± 0.9 (26.8)	16.5 ± 0.7 (17.2)

[a] Load resistance = 100 MΩ. [b] Load resistance = 1 MΩ.

Table S3 Comparison of the power density and stability of conjugated polymers-based TENG previously reported as well as the present work

Reference	Materials	Power density [W m^{-2}]	Stability
[1]	Conjugated microporous polymer (1,3,5-triethynylbenzene with 1,4-diiodoarenes)	8	99.5% of V_{oc} after 30,000 cycles
[2]	Polypyrrole nanowire	8.21	I_{sc} remains at a relatively stable value after 28,800 cycles
[3]	PEDOT:PSS/Ag nanowire	15	No reported
[4]	Polyaniline nanofibers	2.42×10^{-3}	I_{sc} does not significantly reduce after 5,000 s
[5]	Polypyrrole-coated cotton textile	82×10^{-6}	V_{oc} without any noticeable degradation after 5,000 cycles
[6]	PEDOT:PSS	0.2×10^{-3}	Durable and stable device during 8000 cycles
[7]	PEDOT:PSS	4.06×10^{-3}	No reported
[8]	Polyacrylamide-LiCl hydrogel	35×10^{-3}	I_{sc} shows no degradation for 5000 cycles
[9]	Polyacrylamide-LiCl hydrogel	25×10^{-3}	85% of V_{oc} for 5000 cycles
[10]	Polyvinyl alcohol gel	0.4×10^{-6}	V_{oc} shows stable performance for 40,000 cycles
This work	TAP-DPP	2.4	Negligible degradation in V_{oc} after 200,000 cycles

Reference

1. S. I. Park, D.-M. Lee, C. W. Kang, S. M. Lee, H. J. Kim, Y.-J. Ko, S.-W. Kim and S. U. Son, *J. Mater. Chem. A*, 2021, **9**, 12560-12565.
2. S. Cui, Y. Zheng, J. Liang and D. Wang, *Chem. Sci.*, 2016, **7**, 6477-6483.
3. B.-Y. Lee, S.-U. Kim, S. Kang and S.-D. Lee, *Nano Energy*, 2018, **53**, 152-159.
4. S. Cui, Y. Zheng, J. Liang and D. Wang, *Nano Res.*, 2018, **11**, 1873-1882.
5. A. R. Mule, B. Dudem, H. Patnam, S. A. Graham and J. S. Yu, *ACS Sustain. Chem. Eng.*, 2019, **7**, 16450-16458.
6. A. Ahmed, I. Hassan, I. M. Mosa, E. Elsanadidy, G. S. Phadke, M. F. El-Kady, J. F. Rusling, P. R. Selvaganapathy and R. B. Kaner, *Nano Energy*, 2019, **60**, 17-25.
7. Z. Wen, Y. Yang, N. Sun, G. Li, Y. Liu, C. Chen, J. Shi, L. Xie, H. Jiang, D. Bao, Q. Zhuo and X. Sun, *Adv. Funct. Mater.*, 2018, **28**, 1803684.
8. X. Pu, M. Liu, X. Chen, J. Sun, C. Du, Y. Zhang, J. Zhai, W. Hu and Z. L. Wang, *Sci. Adv.*, **3**, 1700015.
9. J. Qi, A. C. Wang, W. Yang, M. Zhang, C. Hou, Q. Zhang, Y. Li and H. Wang, *Nano Energy*, 2020, **67**, 104206.
10. K. Parida, V. Kumar, W. Jiangxin, V. Bhavanasi, R. Bendi and P. S. Lee, *Adv. Mater.*, 2017, **29**, 1702181.